Recent change in surface mass-balance trends of glaciers on James Ross Island, north-eastern Antarctic Peninsula

Zbyněk Engel[1] ![ORCID], Kamil Láska[2], Jana Smolíková[1,2] and Jan Kavan[2,3] ![ORCID]

[1]Faculty of Science, Department of Physical Geography and Geoecology, Charles University, Praha, Czech Republic; [2]Faculty of Science, Department of Geography, Masaryk University, Brno, Czech Republic and [3]Faculty of Science, University of South Bohemia, Centre for Polar Ecology, České Budějovice, Czech Republic

Abstract

Glaciers cover 132 900 km^2 around the Antarctic Ice Sheet, but few are subject to annual mass-balance measurements. Lookalike Glacier and Davies Dome on James Ross Island have been monitored since 2009, providing the third longest mass-balance record for the northern Antarctic Peninsula. These glaciers had a balanced mass budget over the period 2009/10–2014/15 but started to lose their mass thereafter. Between 2014/15 and 2020/21, mass change rates were -0.15 ± 0.13 and -0.26 ± 0.11 m w.e. a^{-1} for Lookalike Glacier and Davies Dome, respectively. The mean equilibrium-line altitudes over this period at Lookalike Glacier (362 ± 18 m a.s.l.) and Davies Dome ($>427 \pm 22$ m a.s.l.) are 51 and >34 m higher compared to the previous 6-year period. The mean accumulation area ratio values determined for the period 2014/15–2020/21 are lower than the balanced-budget ratio indicating that glaciers are out of balance with the current climate. The data confirm the transition from positive to negative mass-balance periods around 2014/15, which is attributed to the change in air temperature trends. The mean summer temperature increased by 0.9°C between the periods 2009/10–2014/15 and 2015/16–2020/21 and melt-season temperatures became predominantly positive.

Introduction

Situated in the north-eastern Antarctic Peninsula, James Ross Island contains more than 100 glaciers, which covered around 1780 km^2 in 2009 (Davies and others, 2012). Mount Haddington Ice Cap, with its outlets, accounts for 80% of the glacierized area of the island coalescing with Dobson Dome in the southern part on the Ulu Peninsula (Fig. 1a). The northern part of Ulu Peninsula, the mostly deglaciated part of James Ross Island, contains small alpine glaciers, which account for <2% of the total glacierized area on island. These glaciers lie 10–30 km from the north-eastern coast of the Antarctic Peninsula and ~73–91 km from its northern tip. Their location on the eastern side of the Antarctic Peninsula, dominated by the ice-bound Weddell Sea, provides a polar continental climate with cold and dry winters and above-freezing summer conditions (Turner and others, 2016; Ambrožová and others, 2020). The near-zero air temperature during the melt season in this region, together with low-elevated accumulation areas and small ice volume renders land-terminating glaciers on the Ulu Peninsula vulnerable to rising temperatures (Davies and others, 2012; Engel and others, 2018). As a result, these glaciers have a short response time and are highly sensitive to air temperature (Davies and others, 2014; Engel and others, 2023), and may provide insights into the recent mass changes of similar small glaciers in the Antarctic Peninsula region. In addition, these glaciers contribute significantly to the runoff of local streams and preserve adjacent fresh water ecosystems, which represent the most important terrestrial habitats of Antarctic life (e.g. Hawes and Brazier, 1991; Kavan and others, 2021).

Due to the remote location of glaciers in the northern part of James Ross Island, little information exists regarding recent changes in their topography and mass balance. However, remote-sensing studies indicate that ice caps, valley and cirque glaciers on the Ulu Peninsula experienced large retreat rates between 1979 and 2006 (Engel and others, 2023 and references therein). These data also indicate that land-terminating glaciers on James Ross Island retreated faster from 1988 to 2001 than between 2001 and 2009 (Davies and others, 2012; Silva and others, 2020). A further decrease in the retreat rates was reported for small glaciers on the Ulu Peninsula (Engel and others, 2019) and for outlet glaciers around James Ross Island (Lippl and others, 2019). A period of reduced retreat rates terminated in the mid-2010s when retreat rates started to increase in the northern part on the Ulu Peninsula (Engel and others, 2019, 2023). The rapid rate of glacier retreat at the end of 20th century is in accordance with a long-term increase in the near surface air temperature (e.g. Vaughan and others, 2003) while the subsequent decelerated retreat reflects the temporary cooling at the turn of the millennium (Turner and others, 2016, 2020; Oliva and others, 2017). The return to a rapid retreat rates after 2015 coincides with a prominent increase in both summer and mean annual air temperature (Engel and others, 2023). Although annual precipitation values were highly variable, winter precipitation increased during the 2010s in the northern part of the Antarctic Peninsula (Carrasco and others, 2021).
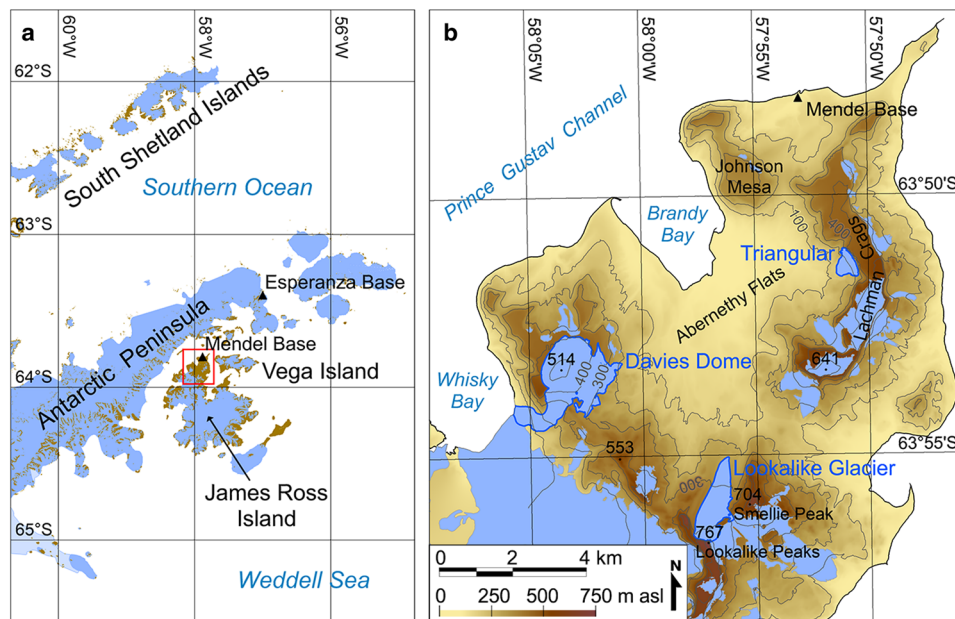
Figure 1. (a) Location of the study area (red rectangle) in the northern Antarctic Peninsula and (b) detailed view of the northern part of James Ross Island, showing the investigated glaciers. Ice-free area on the Antarctic Peninsula after Burton-Johnson and others (2016).

Just two case studies have been published on the surface mass balance (SMB) of the glaciers on James Ross Island. The initial study describes changes in SMB of Davies Dome (Fig. 1b) and Lookalike Glacier (referred to as Whisky Glacier or IJR-45 in previous publications) during the period 2009–15 (Engel and others, 2018), while the second focuses on the effect of air temperatures and snow height changes on the SMB of Triangular Glacier (Engel and others, 2023). The data indicate a predominantly positive SMB until the mass-balance year 2014/15 and persistent glacier mass loss afterwards (Engel and others, 2018, 2022). The change in mass-balance trends around 2015 was attributed to the prominent warming along the eastern coast of the Antarctic Peninsula and the pronounced response of small glaciers to melt-season temperatures (Engel and others, 2023). The sensitivity of these glaciers to air temperature has also been observed elsewhere on the north-eastern side of the Antarctic Peninsula (Abram and others, 2013; Davies and others, 2014; Marinsek and Ermolin, 2015) but their response to precipitation (*sensu* Navarro and others, 2013) remains unknown. Meteorological and glaciological observations on Triangular Glacier have shown that glacier surface decreases mainly by snow melt, but wind transport of snow can be also effective (Engel and others, 2023).

This study aims to reveal the response of small glaciers on James Ross Island to recent atmospheric warming in the northern Antarctic Peninsula region. SMB data collected on Davies Dome and Lookalike Glacier since the mass-balance year 2015/16 are presented and compared with the available SMB records from the northern Antarctic Peninsula region. Recent changes in geometry of these glaciers are assessed using satellite imageries, digital elevation models (DEMs) and ice thickness data derived from a ground-penetrating radar (GPR) survey. Finally, the air temperature records from Johann Gregor Mendel Station (63°48'S, 57°53'W, 10 m a.s.l.; hereafter referred to as Mendel) and Esperanza Base (63°24'S, 56° 59'W, 13 m a.s.l.) weather stations are analysed to connect the observed changes in glacier mass to the mean summer air temperature and number of positive degree-days (PDD).

Study sites

Davies Dome (GLIMS Glacier ID: G301945E63889S), Lookalike Glacier (G302049E63932S) and Triangular Glacier

(G302151E63856S) are located in the predominantly ice-free northern part of James Ross Island, which is situated in the precipitation shadow of the high-elevation (1500–2100 m a.s.l.) plateau regions of the northern Antarctic Peninsula (Fig. 1a). The northern part of James Ross Island, the Ulu Peninsula, is composed of lava-fed delta sequences, which overlie Cretaceous marine sediments (Mlčoch and others, 2019). The sedimentary strata form a low-relief landscape, while the volcanic rocks build prominent cliff-bounded mesa landforms with surfaces at c. 300–600 m a.s.l. (Jennings and others, 2021). Small cold-based ice caps cover the highest parts of these mesas, while headwall cliffs bound the upper part of cirque glaciers (Fig. 1b). The mean annual air temperature is −6.7°C at sea level, but is <−9.0°C at higher-elevation (Ambrožová and others, 2019; Kaplan-Pastíriková and others, 2023). Precipitation is modelled to be between 300 and 700 mm in water equivalent (w.e.) per year (van Wessem and others, 2016; Palerme and others, 2017) but the prevailing south to south-westerly winds strongly affects the distribution of snow cover, transporting snow from flat upper portions of glaciers to their lee sections (Engel and others, 2018; Kavan and others, 2020).

Davies Dome is an ice dome with a flat-topped surface at c. 500 m a.s.l. (Fig. 2a). The dome is located on a volcanic plateau with an elevation of ∼400–450 m a.s.l. and its southern part is drained by a 2.5 km long marine-terminating outlet that terminates in Whisky Bay. In 2010, the maximum ice thickness of the dome determined from GPR data was 83 ± 2 m (Engel and others, 2012). A cumulative mass gain (0.11 ± 0.37 m w.e.) was observed over the period 2009–15 on the dome but the mass change on its sea-terminating outlet remained unknown (Engel and others, 2018).

Lookalike glacier is a valley glacier that is gently inclined (mean slope of 6°) to the NNE. Headwall cliffs and steep slopes bound the upper part of the glacier and its eastern side, respectively. Prominent ice-cored moraines rim the glacier tongue from the north-west (Fig. 2b). The ice thickness of Lookalike Glacier increases towards its central part, where it was measured to be nearly 160 m thick in 2010 (Engel and others, 2012). Over the 2009–15 period, the glacier had a positive cumulative SMB of 0.57 ± 0.67 m w.e. (Engel and others, 2018).

Triangular Glacier is located in the western slope of Lachman Crags plateau at the foot of headwall cliffs that are 120–200 m
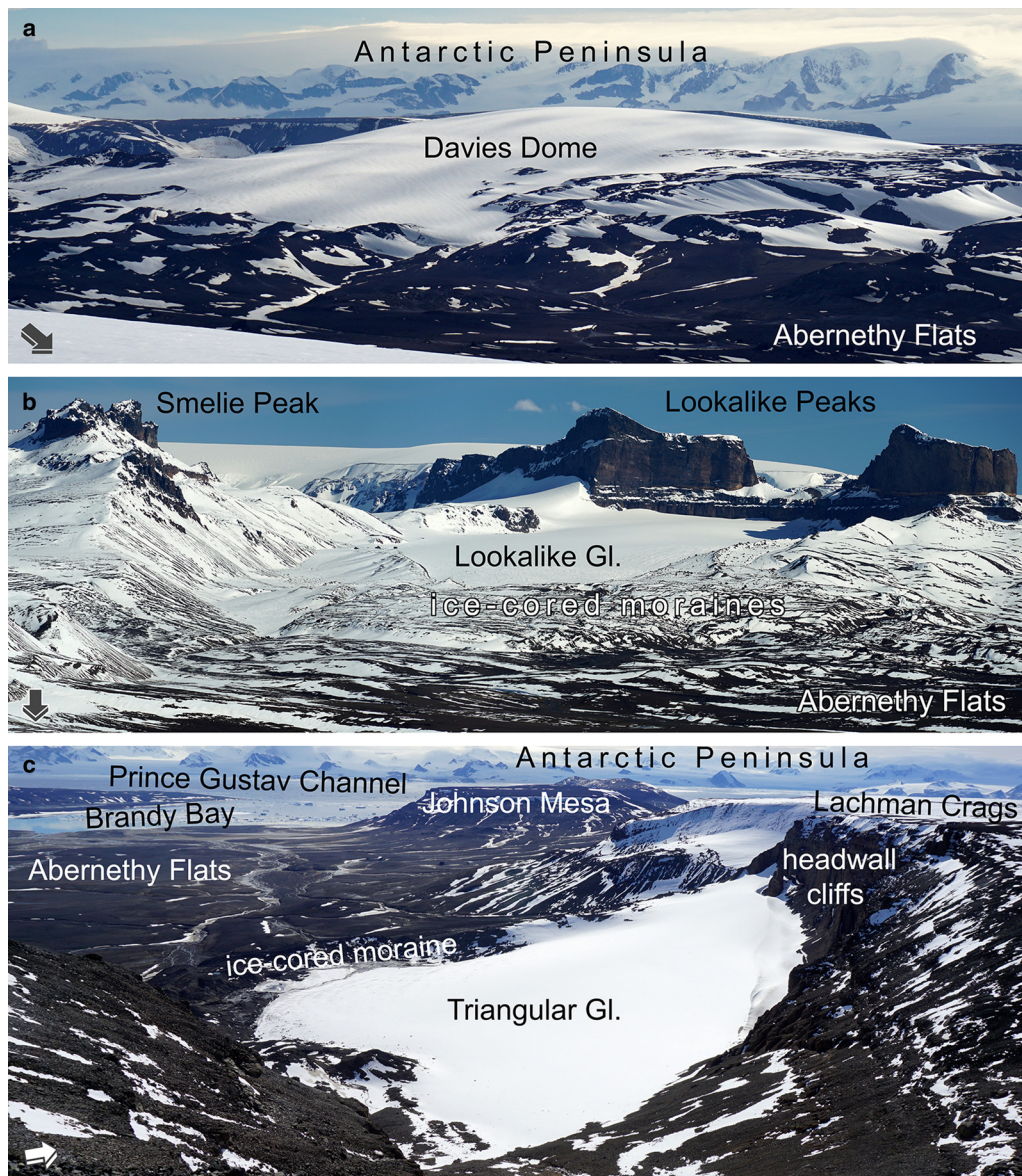
Figure 2. View of (a) Davies Dome from the north-east, (b) Lookalike Glacier from the north and (c) Triangular Glacier from the south-east. See locations in Figure 1. Arrows in the lower left corner of the photos indicate the north direction.

high (Fig. 2c). This cirque glacier is inclined to the south-west and its surface has a mean slope of 15°. Massive ice-cored moraines delimit the north-western margin of the glacier, and more gentle slopes prevail along the glacier's southern boundary. The glacier, with a maximum measured ice thickness of 103 ± 5 m, experienced a cumulative mass loss of -1.66 ± 0.83 m w.e. over the period 2015–2020 (Engel and others, 2023).

Data and methods

Annual mass-balance was measured using the glaciological method between late January and mid-February over the period 2015/16–2020/21 (whenever we refer to the annual mass balance we are specifically referring to the mass-balance year). Observations included the measurement of the height and the position of ablation stakes drilled into the glaciers. The ablation stakes are regularly distributed across the surface of the glaciers except for the crevassed sea-terminating outlet of Davies Dome. Since the mass loss due to frontal ablation of this outlet are not encompassed by the glaciological method, the total mass balance of the entire glacier is less positive or more negative

than the calculated SMB estimate. The inter-annual height differences of the stakes were converted to meters of water-equivalent based on variable density for snow above the equilibrium line and glacier ice in the ablation zone (cf. Huss, 2013). We converted the values in the ablation and accumulation zones using densities of 900 and 500 ± 90 kg m^{-3}, respectively (Engel and others, 2018). As glaciological measurements are made only once a year during the summer, we use this approach assuming that the net elevation difference between subsequent years corresponds to ice and snow in the ablation and accumulation areas, respectively.

Subsequently, we extrapolated point balances over the entire glacier area using the natural neighbour technique (de Smith and others, 2015). This technique was selected as the most appropriate interpolation algorithm for our dataset based on cross-validation results (see Engel and others, 2018 for details). Finally, we quantified uncertainties of the calculated balance values following the recommendations of Huss and others (2009). We applied an uncertainty of ± 90 kg m^{-3} to the snowpack density in the accumulation area to address the uncertainty in the SMB determination at the individual stakes (Engel and others,

2018). The uncertainty that results from spatial interpolation was estimated by the std dev. of the cross-validation residuals obtained from the interpolation of the annual mass-balance grids. The uncertainty in the cumulative SMB was calculated as the square root of the sum of squares of the annual errors for the period 2015/16–2020/21.

Based on the annual mass-balance grids, equilibrium-line altitude (ELA) and accumulation area ratio (AAR) values were determined for the individual mass-balance years within the period 2015/16–2020/21. The ice surface elevation was derived from the Reference Elevation Model of Antarctica (Howat and others, 2019) converted to orthometric heights based on the Earth Gravitational Model 2008 1 min geoid height file (Pavlis and others, 2012). The orthometric (geoid) heights allowed for the comparison of the determined ELAs with the values reported by Engel and others (2018) for the period 2009/10–2014/15. The balanced-budget AAR was estimated based on the relation between the annual SMB and AAR values (Cogley and others, 2011). Mean values of ELA, SMB and AAR are reported with the standard error of the mean.

To evaluate the volume of Davies Dome including its marine-terminating terminus, we analysed the spatial changes of the complete glacier (volume has only been reported for the ice dome by Engel and others, 2012). The position of the glacier front was delineated using WorldView-2/3 and Pléiades imageries from 2015/16 and 2020, respectively, and the ice surface elevation was recorded from the Reference Elevation Model of Antarctica and Pléiades DEM (see the details in Table 1). GPR was used to determine the ice thickness and the volume of both the dome and outlet. The GPR data were collected using an unshielded 50 MHz antenna and RAMAC CU-II control unit (MALÅ GeoScience, 2005). The ice-thickness data retrieved from two-way travel times assuming a radio-wave velocity of $168 \, m \, \mu s^{-1}$ (Narod and Clarke, 1994) were interpolated over the glacier surface using a minimum curvature method (Engel and others, 2012). The uncertainties associated with ice thickness and glacier volume were determined following the recommendations presented by Lapazaran and others (2016a, 2016b) and Martín-Español and others (2016).

Recent changes in the extent and the ice surface elevation of Davies Dome and Lookalike Glacier were assessed based on the 2006 DEM (Czech Geological Survey, 2009) photogrammetrically derived from British Antarctic Survey (BAS) aerial photographs, the Reference Elevation Model of Antarctica and Pléiades DEM (see details in Table 1). The differences between the ice surface DEMs summed with the volume estimates determined from the GPR survey at Lookalike Glacier (Engel and others, 2012) and Davies Dome (Fig. 3) yield the ice volume changes since 2006. The ice-thickness data derived from the GPR survey at Davies Dome were used to model the glacier bed topography following the procedures described by Engel and others (2023). The bed topography was calculated by subtracting the GPR-derived ice-thickness from the Reference Elevation Model of Antarctica surface elevation.

We used the hourly air temperatures from the Mendel station record, which extends back to the beginning of SMB measurements on James Ross Island, as reference climate data. The air temperature was measured at 2 m above the ground using an EMS33H probe and Minikin TH datalogger (EMS Brno, Czech Republic) with an accuracy of ±0.15°C. The hourly values of air temperature were averaged to produce daily, summer (December-January-February) and annual means for the period 2009/10–2020/21. Furthermore, a PDD approach was applied for the surface melt parameterization (Hock, 2003), using hourly air temperature observations. The number of PDD is derived as the integral of the positive air temperature (T) in degrees Celsius (°C) over a selected time interval (A):

$$\text{PDD} = \int_0^A \max\left(T(t), 0\right) \mathrm{d}t| \tag{1}$$

Using Eqn (1), we computed the annual sum of PDD for each mass-balance year and compared it with the annual SMB data.

The long-term climate variability in the northern Antarctic Peninsula was assessed based on the monthly mean air temperatures from Esperanza station (location shown in Fig. 1a) reported in the SCAR MET READER database (Turner and others, 2004). This dataset was used to calculate the mean annual air temperatures and to determine the linear trends for individual decades in the period 1980–2021.

Results

Climate conditions

The mean annual air temperature record from Esperanza station shows a warming through the period 1980–2021 (Fig. 4a). The highest warming trend occurred during the decades 1980–89 (1.33°C decade^{-1}) and 1990–99 (2.60°C decade^{-1}). The temporary cooling followed during the decade 2000–09 (−1.51°C decade^{-1}) that was the coldest period in the northern Antarctic Peninsula region since the 1980s (Fig. 4b). This cooling culminated at the turn of the 2000s when series of low annual temperatures was recorded. During the subsequent decade 2010–19, air temperature started to increase again (1.23°C decade $^{-1}$).

The mean annual air temperature at Mendel station in the northern Ulu Peninsula was −6.6°C in the period 2009/10–2020/21. Air temperature has gradually increased since 2009 (Fig. 5), which can be seen by the increase in mean temperatures between the periods 2009/10–2014/15 (−7.4°C) and 2015/16–2020/21 (−6.1°C). The warmest mass-balance years were 2010/11 and 2016/17, with the mean annual air temperature spanning between −5.7 and −3.9°C. The coldest years were 2009/10 and 2012/13, with the annual means of −8.5 and −8.2°C, respectively.

The mean summer (DJF) air temperature varied throughout the entire period, with a minimum of −1.2°C in summer 2013/14 and a maximum of 1.6°C in summer 2020/21. An increase in the mean summer temperatures, which is most relevant to

Table 1. Summary of the data used in this study

Data source (institution)	Data identification	Acquisition date	Vertical accuracy (m)	Location accuracy (m)	Raster resolution (m)
DEM (CGS) derived from aerial photographs (BAS)	BAS/RN/06	20060214	2.2	0.7	10
Reference elevation model of Antarctica (PGC)	SETSM_WV03_20151012_104001001264D700_1040010011700A00_seg1	20151012	1.95	0.43	2
	SETSM_WV02_20161106_103001005F546900_103001005F6B8D00_seg7	20161106	1.14	0.51	2
Pléiades DEM (CNES)	DS_PHR1B_202001201253228_FR1_PX_W058S64_0101_02249	20200120	1.51	0.47	2

22 ground control points were applied to improve the registration of the Reference Elevation Model of Antarctica strip and Pléiades DEMs.
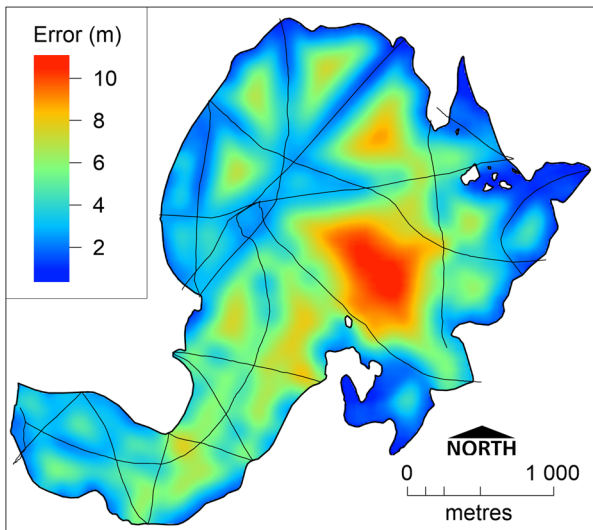
Figure 3. Layout of ground-penetrating radar profiles (black lines) and uncertainty associated with the ice thickness at Davies Dome.

glacier surface melting, was observed between the periods 2009/10–2014/15 (−0.5°C) and 2015/16–2020/21 (0.4°C). There is considerable variability in the annual sum of PDDs, which fluctuates between a minimum of 126.6 K d^{-1} in 2012/13 and a maximum of 354.1 K d^{-1} in 2016/17. The annual PDD sum was almost twice higher in this year compared with the coldest years 2009/10 and 2012/13.

The negative correlation between annual SMB and PDD (Fig. 6) indicates the sensitivity of glaciers to air temperature fluctuations. The glaciers respond more sensitively to summer temperatures as indicated by the linear regression analysis between annual SMB and the summer sum of PDD (Fig. 6b). The higher slope of the regression line obtained for summer PDD implies pronounced changes in glacier mass that occur within the warm period of the year and in the low-altitude zones of the glaciers. The highest correlation was found for Davies Dome ($r = -0.965$), while a slightly lower correlation was calculated for Triangular Glacier ($r = -0.868$). These findings coincide well with the previous studies reporting the high sensitivity of small glaciers on James Ross Island (Davies and others, 2014; Engel and others, 2023) and in adjacent regions of the northern Antarctic Peninsula (Braun and Hock, 2004; Skvarca and others, 2004; Jonsell and others, 2012; Navarro and others, 2023).
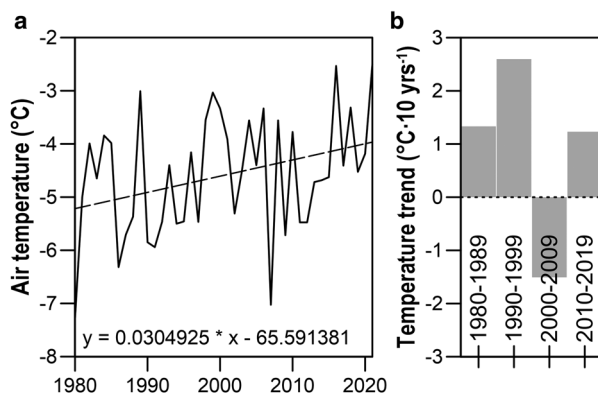
Figure 4. (a) Variation of mean annual air temperature in the period 1980–2021 at Esperanza station and (b) decadal linear air temperature trends. The broken dashed line in panel a shows the linear trend over the entire period. The air temperature data were acquired from the SCAR MET READER surface station database (Turner and others, 2004).
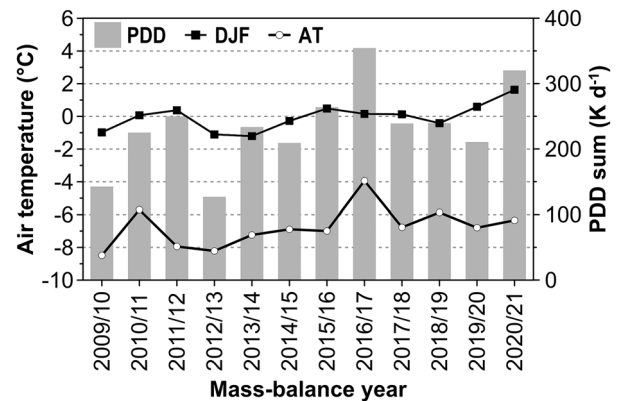
Figure 5. Annual variations in positive degree-days (PDD) sum, mean annual (AT) and summer (DJF) air temperature at Mendel station in the period 2009/10–2020/21.

Glacier area and volume changes

Lookalike Glacier extended over an area of 2.31 ± 0.02 km^2 in 2015, storing 0.2413 ± 0.0136 km^3 of ice. The glacier extent in 2015 was 3.8% smaller compared with the ice area in 2006 (Engel and others, 2012), which represents a mean area loss of 0.010 ± 0.008 km^2 a^{-1} (-0.39% a^{-1}). From October 2015 to January 2020, the glacier extent shrank to 2.29 ± 0.02 km^2 experiencing an area reduction of 1.0% at a mean rate of -0.005 ± 0.013 km^2 a^{-1} (-0.23% a^{-1}). Over this period, Lookalike Glacier lost 0.096 km^3 (0.4%) of ice volume at a mean rate of -0.12% a^{-1}. Its land-terminating glacier front retreated <30 m in total over a period of 4.3 years at a mean retreat rate of 6.8 ± 1.3 m a^{-1} and its mean ice surface elevation slightly decreased (Table 2).

Davies Dome shrank from 6.49 ± 0.03 km^2 in 2006 to 6.27 ± 0.05 km^2 in 2016 (-3.4%) and then to 6.24 ± 0.02 km^2 in 2020 (-0.6%). Its total area reductions were larger than those of Lookalike Glacier but the mean loss rates for the periods 2006–2016 (-0.32% a^{-1}) and 2016–2020 (-0.18% a^{-1}) were comparable to the values obtained for the Lookalike Glacier. The maximum measured ice thickness of 92.3 ± 8.3 m occurs in the middle part of the marine-terminating outlet (at 231 m a.s.l.) of Davies Dome, while the ice dome on a volcanic plateau has the maximum thickness of 88.0 ± 7.4 m (Fig. 7a). The ice volume of Davies Dome decreased by 0.00404 km^3 (1.8%) from November 2016 to January 2020 (-0.56% a^{-1}) mainly due to surface melt. The volume loss due to marine-terminating front retreat accounts for $4.4 \pm 0.4 \times 10^5$ m^3, or 11% of the total ice volume loss. The calving front retreated by 61.0 ± 2.8 m (19.0 ± 1.6 m a^{-1}) and its mean height decreased by 4.1 ± 1.9 m over a period of 3.2 years. The most prominent calving event since the summer 2017/18 occurred on 12 February 2020 (Fig. 8).

Surface mass balance of glaciers

The observed glaciers experienced a negative annual SMB during most of the 6-year period. The land-terminating Lookalike Glacier had a negative balance in 2015/16, near-zero balance in 2016/17, positive balances in 2017/18–2018/19 and negative balances in the last 2 years (Table 3). The surface mass loss culminated in 2020/21 when the most negative annual balance (-0.70 ± 0.32 m w.e.) since 2009/10 was recorded. This negative value contributed substantially to the cumulative SMB of -0.89 ± 0.86 m w.e. over the years 2015/16–2020/21. The highly negative SMB (-0.89 ± 0.62 m w.e.) in 2020/21 was also determined for the neighbouring Triangular Glacier, where the ELA was located above the highest point of the glacier (329 m). This loss added to the past annual balance values (Engel and others, 2023) yields a cumulative
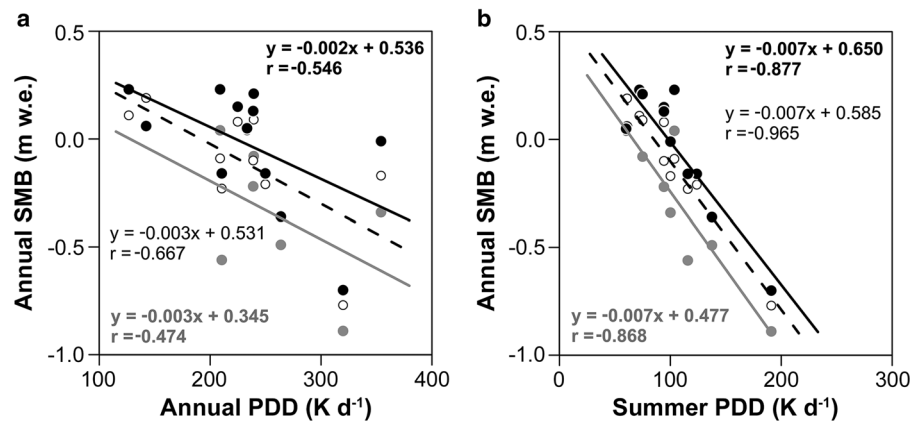
Figure 6. Relation of annual surface mass-balance values (SMB) and (a) annual and (b) summer sum of positive degree-days (PDD) for Lookalike Glacier (black dots and line), Triangular Glacier (grey dots and line) and Davies Dome (white dots and dashed line) over the period 2009/10–2020/21.

SMB of -2.59 ± 0.96 m w.e. over the same 6-year period (the mean ELA was determined to be $>255 \pm 23$ m).

The Davies Dome plateau glacier, which includes a marine-terminating outlet, experienced a net surface mass loss in all years between 2015/16 and 2020/21, except in 2018/19. In the latter year, a slightly positive SMB was determined for both the separate ice dome (0.09 ± 0.16 m w.e.) and the whole glacier including its marine-terminating outlet (0.01 ± 0.30 m w.e.). As the rest of the investigated land-based glaciers on James Ross Island, Davies Dome experienced the largest surface mass loss in 2020/21 for both the separate ice dome (-0.77 ± 0.15 m w.e.) and for the complete glacier with outlet (-0.83 ± 0.19 m w.e.). A surface lowering was recorded at all the ablation stakes in this particular year, which is the first year since the beginning of the mass-balance measurements in 2009 with zero AAR and ELA above the upper glacier limit (Table 3). A cumulative SMB of -1.55 ± 0.60 m w.e. was calculated for Davies Dome (without its outlet) over the period 2015/16–2020/21.

The mean surface mass loss of 0.26 ± 0.11 m w.e. a^{-1} measured for Davies Dome represents the ice dome only. The marine-terminating outlet decreases the annual SMB values by 0.10–0.06 m w.e. (Table 2) and further losses arise from iceberg calving and submarine melting at the glacier front. Frontal ablation remains unknown but the mean annual volume loss due to ice front retreat from 2015/16 to 2019/20 was 0.14 ± 0.01 million m^3, or 0.06 m w.e. Considering this value for the years 2015/16–2020/21, the mass loss of the complete glacier exceeds 0.4 ± 0.2 m w.e. a^{-1}. The volume loss due to frontal retreat accounts for 13–29% of the surface mass loss of Davies Dome and implies the minimum contribution of frontal ablation assuming low ice surface velocities and small number of calving events observed at the glacier terminus. If we consider the similar contribution of both the surface and frontal ablation in the northern Antarctic Peninsula region (Navarro and others, 2013; Osmanoğlu and others, 2014), the total mass loss of Davies Dome with its outlet increases to 0.7 ± 0.2 m w.e. a^{-1}.

A west–east gradient in SMB dominated the annual mass-balance spatial distribution on Lookalike Glacier over most of the investigated period (Fig. 9). A less pronounced asymmetric pattern was observed in 2016/17 and 2019/20, when SMBs were close to zero and the SMB distribution was largely controlled by elevation (Figs 9b, e). The SMB distribution of Davies Dome was more complicated, with increasing mass loss towards the periphery of the dome (i.e. elevation controlled SMB) only observed in the markedly negative mass-balance year of 2020/21 (Fig. 10f). In all the previous years between 2015/16 and 2019/20, the SMB increased along the SW–NE transect attaining positive values on the north-eastern slope of the dome (Figs 10a–e).

Equilibrium-line altitude

The annual ELA determined for Lookalike Glacier ranged between 310 and 378 m except for 2020/21, when enhanced ablation raised it to 449 m (Table 3). The equilibrium line was nearly parallel to contours in 2016/17 only (Fig. 9b). In the rest of the period, it had a complex spatial pattern and crossed several contour lines. The annual values yielded a mean ELA of 362 ± 18 m over the 6-year period. The AAR values ranged from 0.71 to 0.02, with an average of 0.42 ± 0.10. At Davies Dome, the annual ELA ranged from 335 to 438 m before the last year, when the ablation zone expanded across the entire glacier (Fig. 10f). Including the very high ELA of 2020/21, which was above the maximum altitude (519 m) of the glacier, the arithmetic mean of the six annual values yields a value of 427 ± 22 m. AAR was often quite low, with a value of zero in 2020/21, and nearly-zero in 2015/16 and 2019/20. Combined with the remaining annual values, AAR was, on average, 0.24 ± 0.11. The relation between the SMB and AAR, observed over 12 years, indicates the balanced-budget AAR of 0.58 and 0.48 for Lookalike Glacier and Davies Dome, respectively.

The mean ELA over the period 2015/16–2020/21 was 51 and >34 m higher compared with the previous 6-year period at Lookalike Glacier and Davies Dome, respectively (Table 4). The observed shift in ELA follows an increase in the mean summer air temperature of 0.9℃ on the glaciers between the 6-year periods. Despite this shift, the current ELA probably remains lower compared with the period 2005–09 when the mean summer air temperature on the Ulu Peninsula was 0.3℃ higher

Table 2. Spatial characteristics of Davies Dome, Lookalike Glacier and Triangular Glacier

Glacier	Latitude/longitude	Elevation (m a.s.l.)	Year	Length (km)	Mean elevation (m a.s.l.)	Area (km²)	Volume (km³)
Davies Dome	63°55′00″–63°56′42″ S	0–514	2016	3.391	348.2 ± 1.1	6.27 ± 0.05	0.226 ± 0.010
	57°56′05″–57°57′53″ W		2020	3.333	349.4 ± 0.5	6.24 ± 0.02	0.222 ± 0.011
Lookalike Glacier	63°52′39″–63°54′30″ S	218–547	2015	3.155	345.5 ± 2.0	2.31 ± 0.02	0.241 ± 0.014
	58°00′54″–58°05′44″ W		2020	3.126	345.4 ± 1.6	2.29 ± 0.02	0.240 ± 0.011
Triangular Glacier	63°51′01″–63°51′35″ S	104–329	2016	0.801	190.8 ± 4.5	0.55 ± 0.02	0.026 ± 0.001
	57°50′26″–57°51′25″ W		2020	0.797	189.7 ± 4.2	0.54 ± 0.02	0.025 ± 0.001
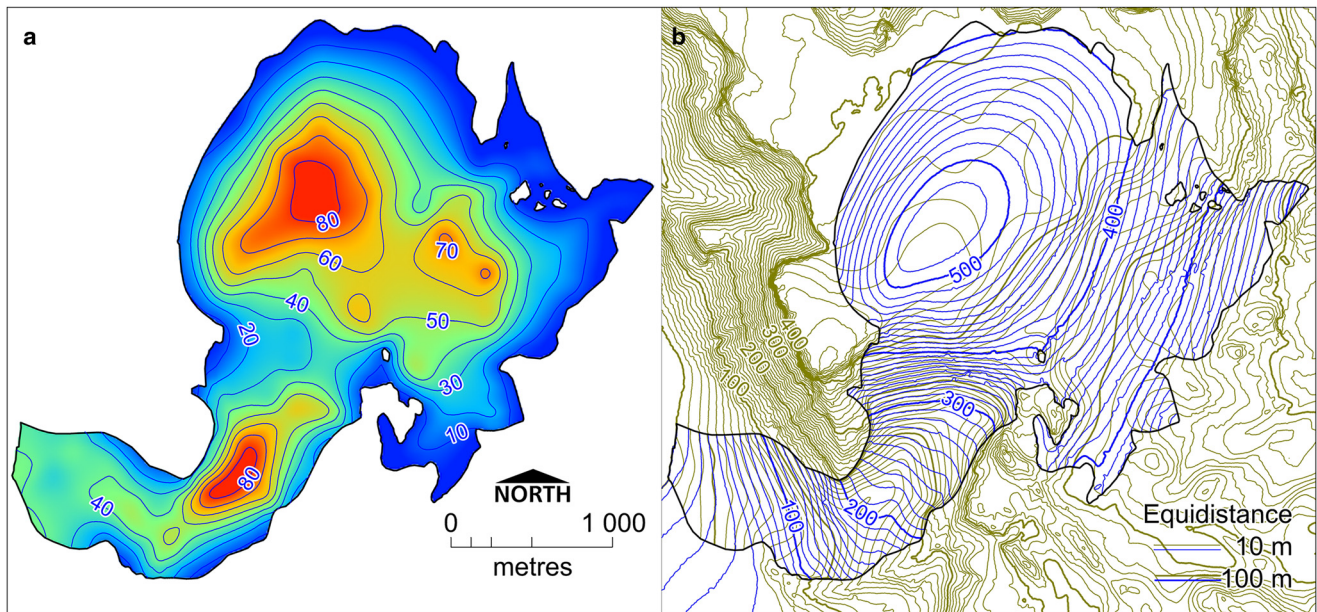
Figure 7. (a) Ice thickness in 2018 and (b) glacier surface/bed elevations of Davies Dome.

(Ambrožová and others, 2019). Furthermore, it equals the regional ELA at the turn of the millennium when the temporary cooling phase initiated (Turner and others, 2016). The mean AAR decreased between the periods 2009/10–2014/15 and 2015/16–2020/21 by 0.26 and 0.2 at Lookalike Glacier and Davies Dome, respectively. As a result, the mean AAR values for the recent 6-year period are lower than the balanced-budget AAR indicating that glaciers are out of balance with the current climate conditions. This implies further glacier retreat and volume loss if the current climate conditions in the region persist.

An extreme surface ablation occurred on the investigated glaciers during the summer of 2020/21. Enhanced melt expanded to the upper part of Lookalike Glacier causing slush swamps and sheet flows below the snow-covered ice divide. Open cryoconite holes formed at an exceptional elevation of 440 m a.s.l., and supraglacial channels (hundreds of meters long and up to 1 m deep) emerged along both margins of the glacier. At the same time, snow cover melted over 100% of Triangular Glacier exposing glacier ice to melt conditions and prompting surface meltwater runoff across the glacier. Finally, surface melt extended across the entire flat top surface of Davies Dome (∼500 m a.s.l.), which is normally a dry snow zone. The meltwater was partly retained within the snowpack, but it eventually flowed from the percolation zone forming supraglacial stream networks on the north-eastern slope of the dome and on the marine-terminating outlet.

Discussion

Accelerated glacier mass loss

The retreat rates determined for Lookalike Glacier and Davies Dome indicate regional changes in glacier evolution at the beginning of the 21st century. In 2015/16, the glaciers remained close to their 2006 extent experiencing reductions of 3.8% ($-0.4\%\,a^{-1}$) and 3.4% ($-0.3\%\,a^{-1}$) over the period 2006–2015/16. These values coincide with that determined for Triangular Glacier (3.2% and $-0.3\%\,a^{-1}$), being an order of magnitude lower compared with the reductions reported for Lookalike Glacier (10.6%), Davies Dome (20.7%) and Triangular Glacier (30.8%) over the period 1979–2006 (Engel and others, 2012, 2023). The ongoing decrease of area loss ($-0.2\%\,a^{-1}$) derived for both Lookalike Glacier and

Davies Dome over the period 2015/16–2020, and the accelerated retreat of Triangular Glacier ($-0.9\%\,a^{-1}$), indicate a shift in glacier evolution around the mid-2010s (Fig. 11). This shift is also demonstrated by changes in the rates of glacier volume loss, that nearly doubled between the periods 2006–2015/16 (0.1 to $-0.3\%\,a^{-1}$) and 2015/16–2020 (-0.1 to $-0.6\%\,a^{-1}$). The timing of the shift is also constrained with the glaciological measurements, which yield predominantly negative annual SMBs of the observed glaciers since 2015/16. The surface mass loss over the period 2015/16–2020/21 is higher than the surface mass gain over the previous 8-year interval (Table 4).

The observed shift towards mass loss indicates a change in the mass balance of the investigated glaciers. However, uncertainty in the annual SMB values and the short observation period do not allow statistically significant trend to be determined. Nevertheless, the recent onset of enhanced glacier mass loss, directly following a sustained period of increased air temperatures, implies that the previous period of reduced warming and mass losses (Turner and others, 2016; Oliva and others, 2017) has terminated. Increased air temperatures since the mid-2010s (Carrasco and others, 2021) and enhanced temperature-controlled processes such as surface snow melt (Zheng and others, 2019; Zhou and others, 2021) and glacier ablation (Engel and others, 2023; WGMS, 2023) in the north-eastern Antarctic Peninsula indicate a return to a long-term positive trends in air temperature (e.g. Turner and others, 2020), snow melt (Abram and others, 2013) and ice mass loss (Carrivick and others, 2012). However, mass loss of the glaciers on the Ulu Peninsula is driven by summer temperatures (Engel and others, 2023) that are related to the highly variable phase of the Southern Annular Mode (Marshall and Thompson, 2016) and, therefore, short-term periods of less negative or positive mass balances are still possible in the upcoming years. Ongoing atmospheric warming, and enhanced glacier retreat and thinning observed on James Ross Island since 2020/21 corroborate our hypothesis of a return to the long-term negative mass-balance trend.

The largest losses of ice volume determined for Davies Dome result from surface melt and frontal ablation at the marine-terminating outlet. Higher volume losses of marine-terminating glaciers compared to land-terminating ice masses were observed around the northern Antarctic Peninsula, but ocean-calving
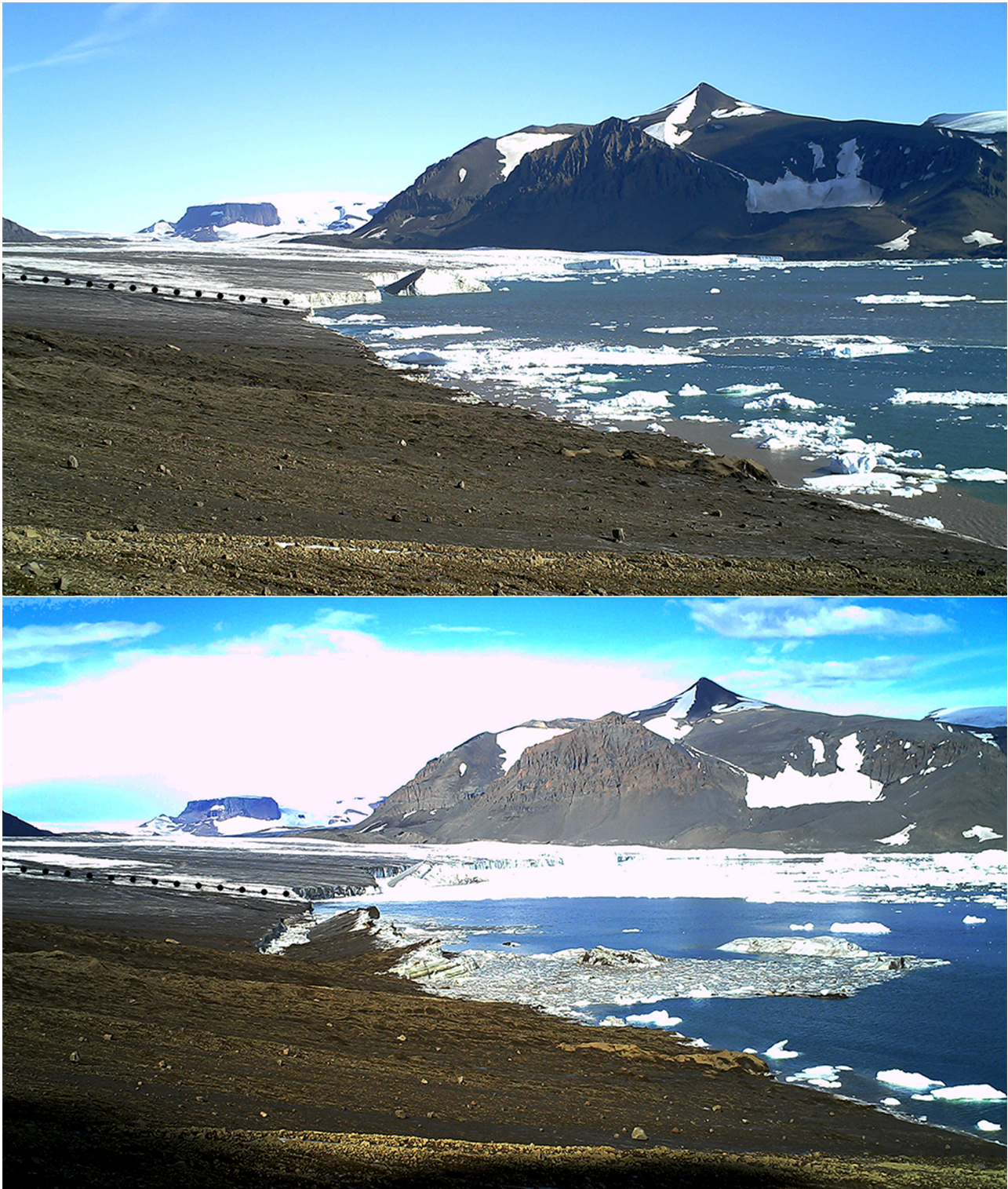
Figure 8. Calving event at marine-terminating margin of Davies Dome outlet in Whisky Bay on 12 February 2020. Dashed lines indicate connection of Davies Dome (in front) and Whisky Glacier termini.

glaciers have been considered much more dynamic (Skvarca and others, 1995; Carrivick and others, 2012; Cook and others, 2014). The limited changes of Davies Dome may be attributed to the location of its accumulation zone at a relatively high elevation (>400 m a.s.l.), short floating section of its outlet (200–700 m) and narrow terminus (325 m or >2% of the glacier perimeter) affected by calving (Fig. 7b). By contrast, marine-terminating outlets on James Ross Island are mostly kilometres long and wide (Lippl and others, 2019) being more vulnerable to reduced sea-ice extent in the Weddell Sea (Parkinson, 2019) and related changes

in air temperature (Turner and others, 2020; Carrasco and others, 2021).

The increased mass loss observed on the Ulu Peninsula since 2015/16 corresponds with the onset of negative annual SMBs determined for Bahía del Diablo Glacier on Vega Island, the north-eastern Antarctic Peninsula (Fig. 12). One year later, the shift to accelerated mass loss was observed on glaciers on the South Shetland Islands north from the Peninsula (WGMS, 2021). The timing of the change in mass-balance trends around the northern Antarctic Peninsula is consistent with the

Table 3. Annual values of surface mass balance (SMB), equilibrium-line altitude (ELA) and accumulation area ratio (AAR) for Lookalike Glacier and Davies Dome during the mass-balance years 2015/16–2020/21
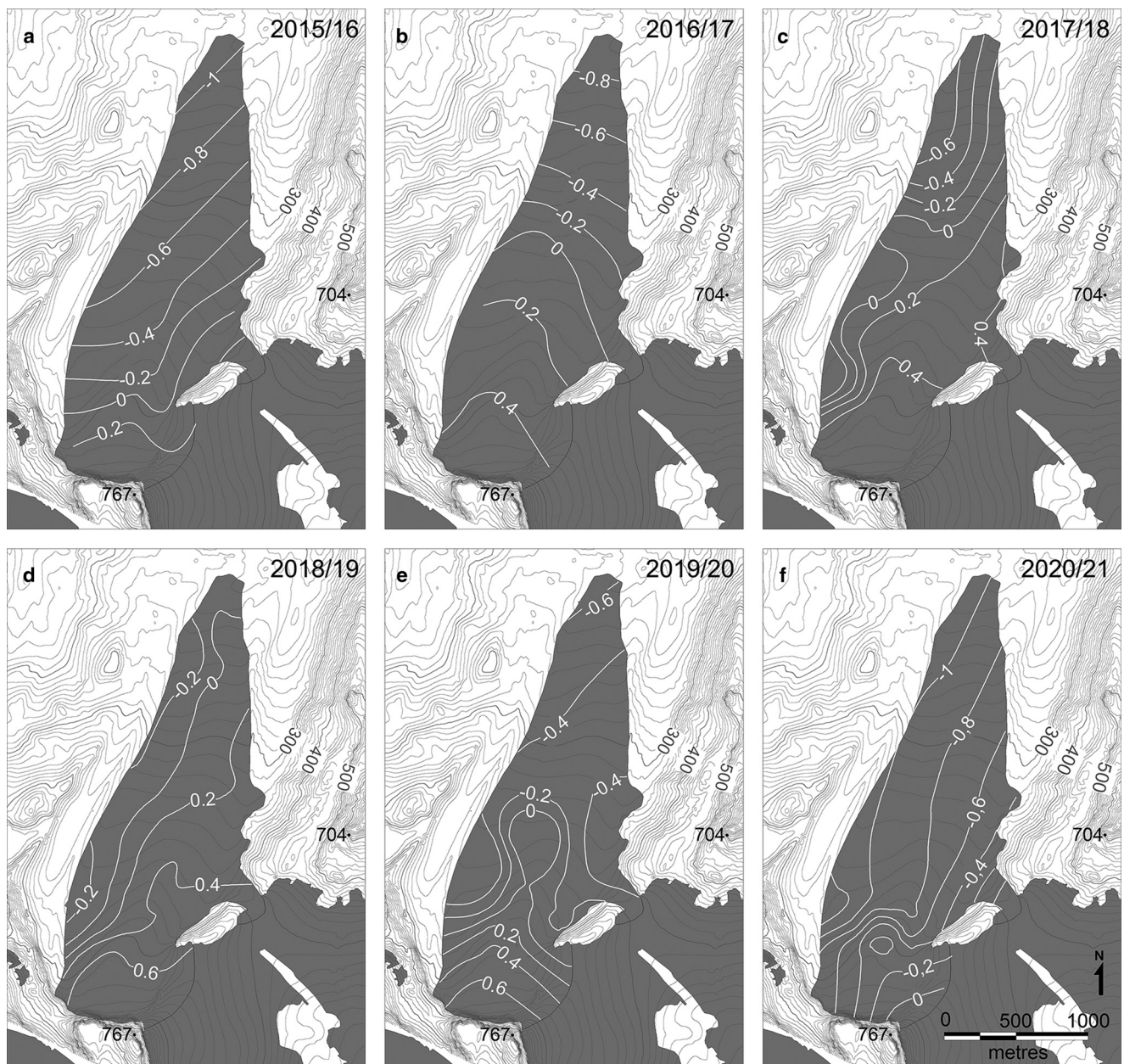
| Mass-balance year | Lookalike glacier | | | Davies Dome with outlet | | | |
	SMB (m w.e.)	ELA (m)	AAR	SMB (m w.e.)	SMB (m w.e.)	ELA (m)	AAR
2015/16	−0.36 ± 0.39	378	0.24	−0.36 ± 0.28	-	424	0.07
2016/17	−0.01 ± 0.39	336	0.57	−0.17 ± 0.38	-	448	0.29
2017/18	0.13 ± 0.36	333	0.65	−0.10 ± 0.25	-	402	0.32
2018/19	0.21 ± 0.28	310	0.71	0.09 ± 0.16	0.01 ± 0.30	335	0.75
2019/20	−0.16 ± 0.36	368	0.28	−0.23 ± 0.16	−0.33 ± 0.27	436	0.02
2020/21	−0.70 ± 0.32	449	0.02	−0.77 ± 0.15	−0.83 ± 0.19	>519	0.00

acceleration of glaciers on the eastern and western Antarctic Peninsula (Tuckett and others, 2019; Wallis and others, 2023). Increased ice loss since 2017 has been reported for Pine Island and Thwaites glaciers in the Amundsen Sea sector of West Antarctica (Joughin and others, 2021; Surawy-Stepney and others, 2023). Irrespective of the unique climate conditions in Antarctica, recently accelerated global glacier mass loss has been detected in most of the glacierized regions around the world (Hugonnet and others, 2021).

Glacier–climate interaction

The observed changes in the glacier extent are consistent with the air temperature record from Esperanza station (Figs 4b, 11). The

Figure 9. Spatial distribution of the annual surface mass balance (in m w.e.) of Lookalike Glacier during the period 2015/16–2020/21.
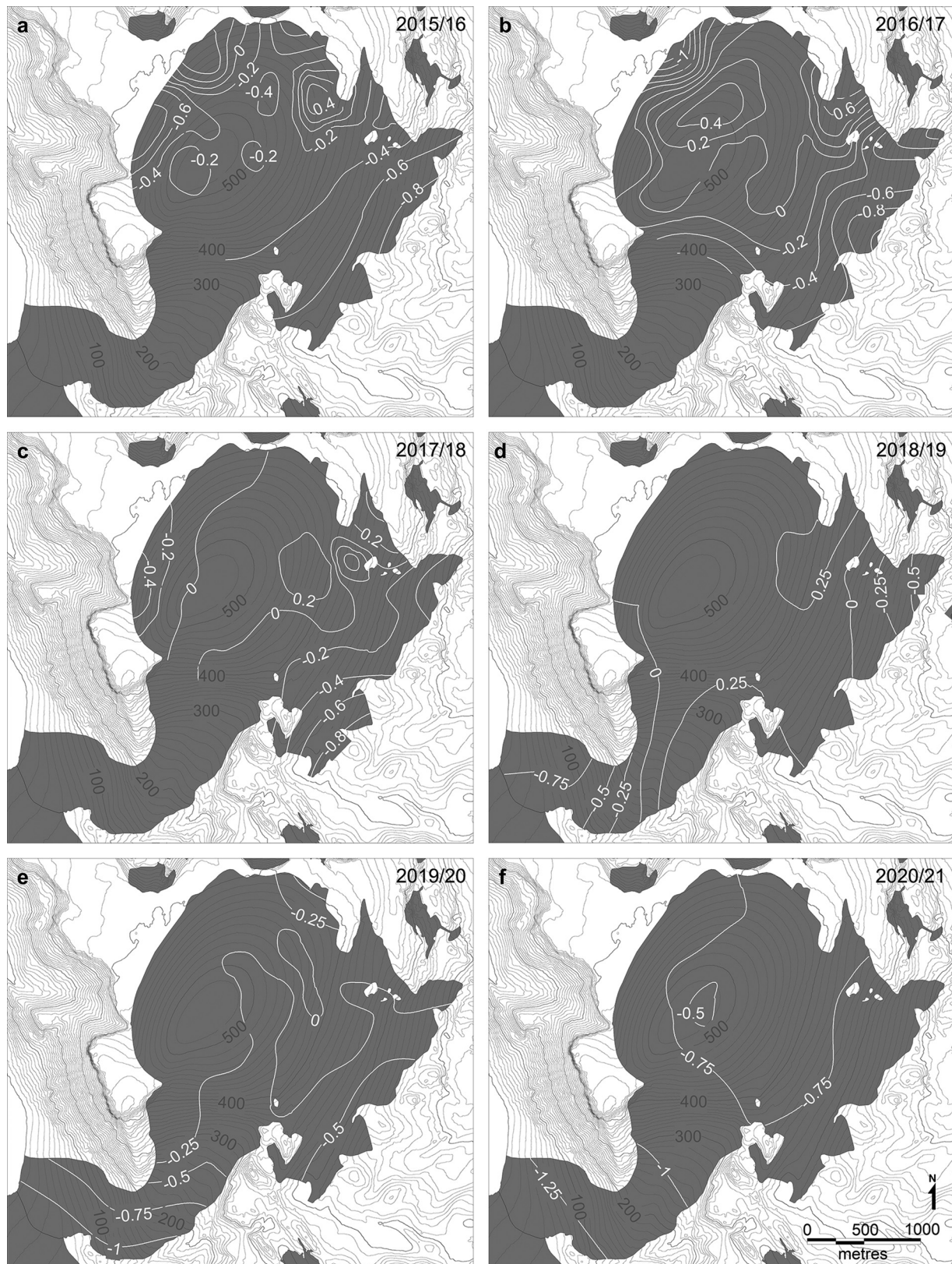
Figure 10. Spatial distribution of the annual surface mass balance (in m w.e.) of Davies Dome during the period 2015/16–2020/21.

largest retreat rates reported by Engel and others (2012, 2023) for the period 1979–2006 coincide with the most prominent temperature increase in the Antarctic Peninsula region prior 1999 (e.g. Vaughan and others, 2003; Turner and others, 2005; Jones and others, 2019). The subsequent decrease in retreat rates observed over the period 2006–2015/16 resulted from cold conditions

during the 2000s. This temporary cooling and its consequences for glacier melting in the northern Antarctic Peninsula were reported by Navarro and others (2013) and Oliva and others (2017).

The cooling phase on Ulu Peninsula culminated between 2012 and 2014 when cold summer conditions, with the mean summer

Table 4. Mass-balance characteristics for the investigated glaciers over the period 2009/10–2020/21

Glacier	Characteristic	2009/10–2014/15	2015/16–2020/21	2009/10–2020/21
Lookalike Glacier	Cumulative SMB (m w.e.)	0.57 ± 0.67	−0.89 ± 0.86	−0.33 ± 1.09
	Mean annual SMB (m w.e.)	0.09 ± 0.05	−0.15 ± 0.13	−0.03 ± 0.08
	ELA (m)	311 ± 16	362 ± 18	343 ± 14
	AAR	0.68 ± 0.09	0.42 ± 0.10	0.51 ± 0.08
Davies Dome without outlet	Cumulative SMB (m w.e.)	0.11 ± 0.37	−1.55 ± 0.60	−1.44 ± 0.70
	Mean annual SMB (m w.e.)	0.02 ± 0.05	−0.26 ± 0.11	−0.12 ± 0.07
	ELA (m)	393 ± 18	>427 ± 22	>412 ± 14
	AAR	0.44 ± 0.09	0.24 ± 0.11	0.31 ± 0.07
Triangular Glacier	Cumulative SMB (m w.e.)	-	−2.59 ± 0.96	-
	Mean annual SMB (m w.e.)	-	−0.43 ± 0.10	-
	ELA (m)	-	>255 ± 23	-
	AAR	-	0.19 ± 0.08	-

Data for the period 2009/10–2014/15 after Engel and others (2018).

air temperature of <−1.0°C, reduced seasonal ablation and annual surface mass gains. The subsequent temperature increase resulted in considerably warmer conditions during the period 2015/16–2020/21 as indicated by predominantly positive mean summer temperatures and 1.3°C higher mean annual temperature compared with the mean for the previous 6-year period. The observed increase in the annual and summer air temperatures coincides with the acceleration of warming (Carrasco and others, 2021) and more frequent heat waves across the Antarctic Peninsula (González-Herrero and others, 2022). In addition to the warming trend, an increase in rainfall events in the northern part of the Peninsula since 2014 (Carrasco and others, 2020) contributed to glacier surface melting.

Whereas glacier surface melting varies from year to year with summer temperature, snow accumulation (a major positive component of SMB), is a function of precipitation. In situ measurements of precipitation using a disdrometer have been initiated at Mendel station in the summer 2020/21 and numerical modelling remains the only source of information about local precipitation (Matějka and Láska, 2022). The model simulates small precipitation increase in the northern part of James Ross Island over the period 1979–2014 (1–3 mm w.e. a^{-2}), but without a significant trend (van Wessem and others, 2016). At regional scale, precipitation records are available from O'Higgins station in the northern part of Antarctic Peninsula and from Frei and Prat stations located on the South Shetland Islands. These station records have revealed a large year to year variability of precipitation amounts, an increase in precipitation around the northern Antarctic Peninsula since 2000, and the largest positive trend of winter precipitation over the last 10 years (Carrasco and Cordero, 2020). The strong variability in precipitation is

consistent with modelled results by van Wessem and others (2016), but biases remain in the identified trends over the northern Antarctic Peninsula.

The distribution of cumulative SMB on the glaciers (Fig. 13) confirms the significance of snowdrift and redistribution by wind on the glacier mass changes. The wind-driven changes in the distribution of snow were suggested as a reason for the differences in the surface mass gain in the accumulation zones of Davies Dome and Lookalike Glacier (Engel and others, 2018). The removal of snow and its effect on the mass-balance pattern was recently reported for Triangular Glacier (Engel and others, 2022). A shift of the accumulation area on Davies Dome to its north-eastern slope (Fig. 13b) confirms the significance of snowdrift for SMB of small glaciers in the Antarctic Peninsula region (Navarro and others, 2013). The accumulation zone covered almost the entire dome over the cold period 2009/10–2014/15 but moved to its lee-side surface during the subsequent years when negative SMB prevailed. Despite the north-eastern aspect of this surface being directly exposed to solar radiation, the
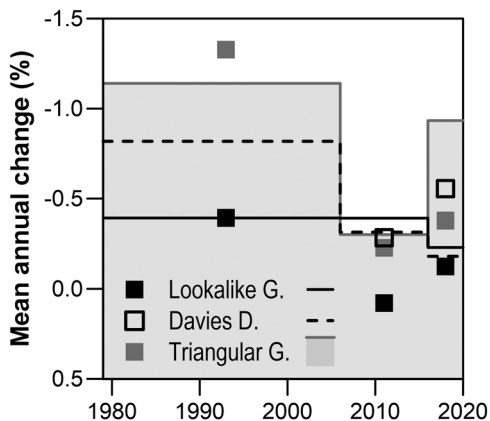
Figure 11. Mean annual change in area (lines) and volume (squares) of the investigated glaciers over the period 1979–2020.
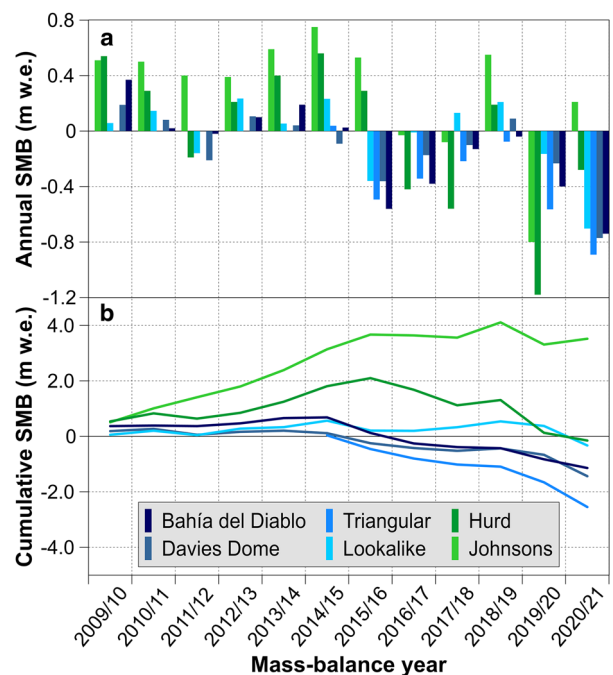
Figure 12. (a) Annual and (b) cumulative surface mass-balance values of selected glaciers in the northern Antarctic Peninsula region since the mass-balance year 2009/10. Green colours represent glaciers on South Shetlands Islands (north-western side of the Peninsula), whereas dark blue shows Bahía del Diablo Glacier on Vega Island and lighter blue shades mark glaciers on James Ross Island (north-eastern side). Data for Bahía del Diablo, Hurd and Johnsons Glaciers from the WGMS (2021).
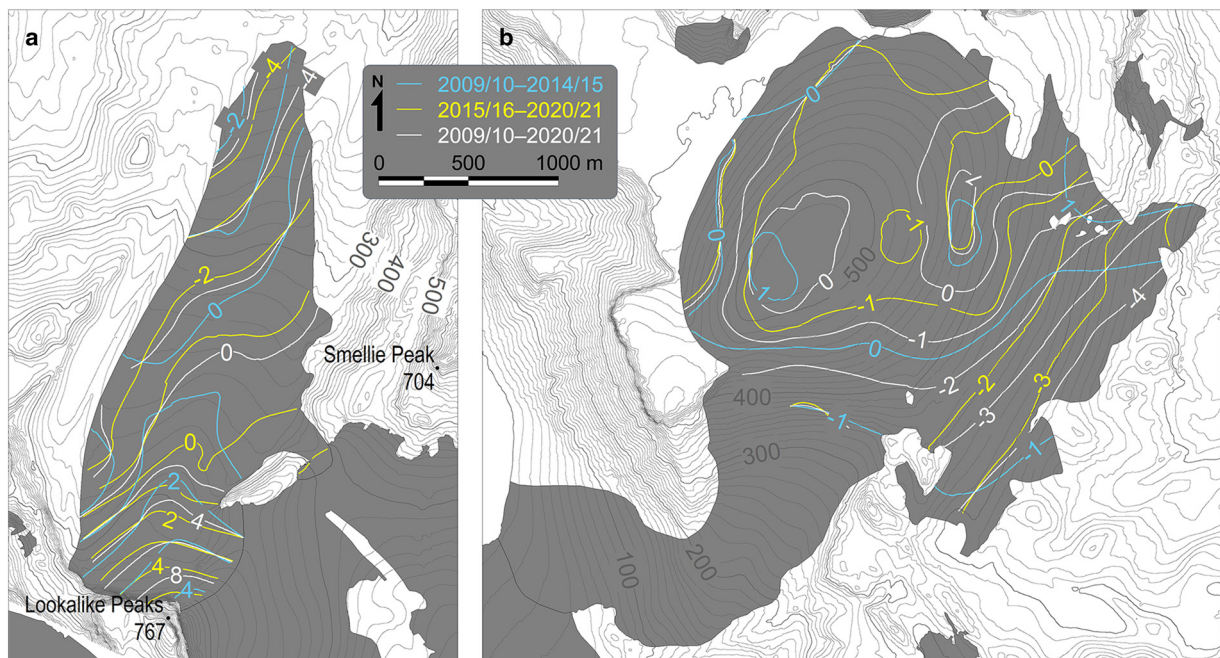
Figure 13. Spatial distribution of the cumulative surface mass balance (in m w.e.) of (a) Lookalike Glacier and (b) Davies Dome over the periods 2009/10–2014/15, 2015/16–2020/21 and 2009/10–2020/21.

accumulation of snow is enhanced by south-westerly winds (Kavan and others, 2020). As a result, the accumulation zone of Davies Dome was not located on the coldest flat top of the dome but at surfaces with the highest accumulation of snow. The lee-side factor prevails in the SMB distribution on the glacier over the complete observation period 2009/10–2020/21, though the effect of the altitude remains visible as a minor accumulation zone at the highest part of the dome.

Implications of the observed changes

Significant relationships between the annual values of the SMB, ELA and AAR (Fig. 14) indicate that all these variables can be used to analyse the impacts of climate conditions on the investigated glaciers. The plots of SMB versus ELA and AAR reflect higher climate sensitivity of Triangular Glacier that has narrow accumulation zone in its upper section and more simple geometry than Lookalike Glacier and Davies Dome. The lower ELA determined for Triangular Glacier (Table 4) and the higher slope of the regression line obtained for its AAR (Fig. 14b) imply pronounced changes in glacier mass under less extreme climate perturbations. The location of this cirque glacier at a low elevation

range suggests that its ELA will rise more frequently in the future above the upper limit of the glacier, implying its earlier disappearance compared with Lookalike Glacier and Davies Dome (Engel and others, 2023). Triangular Glacier is the smallest ice mass in the Antarctic periphery subject to annual glaciological measurements and represents a category of glaciers that is most vulnerable to regional atmospheric warming (e.g. Simões and others, 2004; de Woul and Hock, 2005; Huss and Fischer, 2016).

Despite the larger ice volume of Davies Dome and its relatively low rate of mass loss, its gently sloped accumulation area renders this glacier particularly susceptible to possible future rises in ELA. It has been suggested that glaciers with low-lying ablation areas and large flat accumulation areas could lose their accumulation area rapidly under rise in ELA (Davies and others, 2012). The SMB measurements on Davies Dome document the validity of this view as an increase of ~35 m in mean ELA between the periods 2009/10−2014/15 and 2015/16−2020/21 resulted in 90% loss of accumulation area (Figs 13, 15). Further rises in ELA would probably speed-up surface melt considerably through the ice dome thinning and related enhanced reduction of accumulation area. The mass-balance modelling suggests that extreme negative mass-balance rates can be expected on ice cap-like glaciers which
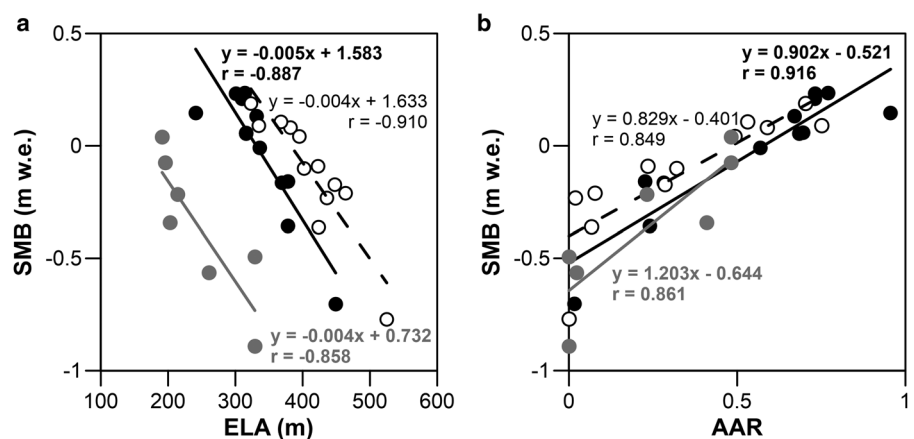
Figure 14. Annual surface mass-balance values (SMB) versus (a) equilibrium-line altitude (ELA) and (b) accumulation area ratio (AAR) for Lookalike Glacier (black dots and line), Triangular Glacier (grey dots and line) and Davies Dome (white dots and dashed line) over the period 2009/10–2020/21.
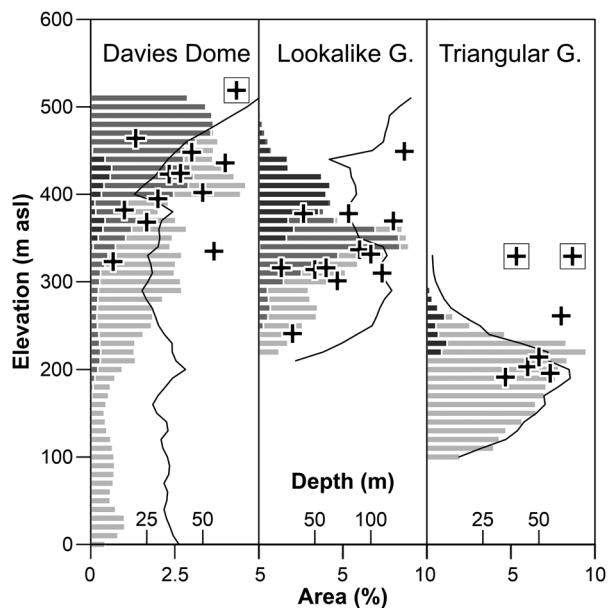
Figure 15. Area–altitude distribution (light grey bars) in 2020 and mean ice thickness for altitude bands (solid line). Medium and dark grey bars represent accumulation areas over the period 2009/10–2014/15 and 2015/6–2020/21, respectively. Crosses indicate series of annual equilibrium-line altitudes determined since the glaciological year 2009/10 (Davies Dome and Lookalike Glacier) and 20145/15 (Triangular Glacier). Rectangles mark annual ELAs above the upper limit of the glaciers.

Irrespective of their contribution to sea-level change, small glaciers cover most Antarctic islands and represent unique ecosystem (Anesio and Laybourn-Parry, 2012). Moreover, melt-water discharge from these glaciers has a significant impact on the development of terrestrial ecosystems (Jung and others, 2022) and deglaciated landscape (Ruiz-Fernández and others, 2019).

Conclusions

Lookalike Glacier and Davies Dome in the northern part of James Ross Island have lost their ice volume at an accelerated rate since 2015. After a period of reduced glacier retreat between 2006 and 2015, the land-terminating Lookalike Glacier lost $-0.1\% \, a^{-1}$ of its volume from October 2015 to January 2020 and Davies Dome, together with its marine-terminating outlet, shrank in volume by $-0.6\% \, a^{-1}$ between November 2016 and January 2020. The mean annual volume loss due to calving front retreat over a period of 4.3 years was estimated to be $1.4 \pm 0.1 \, 10^5 \, m^3$, or 11% of the total volume loss from Davies Dome.

Lookalike Glacier and Davies Dome experienced a surface mass loss of -0.89 ± 0.86 and -1.55 ± 0.60 m w.e., respectively, losing mass at the mean rate of -0.15 ± 0.13 and -0.26 ± 0.11 m w.e. a^{-1}. Surface mass loss for the period 2015/16–2020/21 exceeds the surface mass gain reported for the previous 6-year period resulting in negative cumulative SMBs over the years 2009/10–2020/21 for both Lookalike Glacier (-0.33 ± 1.09 m w.e.) and Davies Dome (-1.44 ± 0.70 m w.e.). The mean annual SMBs over the period 2015/19–2020/21 were -0.15 ± 0.13 m w.e. for Lookalike Glacier and -0.26 ± 0.11 m w.e. for Davies Dome.

The mean ELAs at Lookalike Glacier (362 ± 18 m a.s.l.) and Davies Dome ($>427 \pm 22$ m a.s.l.) during the period 2015/16–2020/21 were 51 and >34 m higher compared with the period 2009/10–2014/15. Between these 6-year periods, the mean AAR for Lookalike Glacier and Davies Dome decreased from 0.68 ± 0.09 to 0.42 ± 0.10 and from 0.44 ± 0.09 to 0.24 ± 0.11, respectively. The mean AARs are lower than the balanced-budget ratio values, which indicate that the glaciers are out of balance with the current climate conditions.

The transition from the surface mass gain to mass loss around 2014/15 is attributed to the changes in the near surface air temperature trends in the region. The mean annual temperature increased from $-7.4°C$ in the period 2009/10–2014/15 to $-6.1°C$ in the period 2015/16–2020/21. This enhanced rate of mass loss reflects warmer melt-season conditions in the latter period, which had both mean summer air temperature ($+0.9°C$) and PDD sum ($+33.1$ K) higher compared with those of the period 2009/10–2014/15. The high sensitivity of the investigated glaciers to air temperature changes in the Antarctic Peninsula region confirms their vulnerability to the acceleration of regional warming associated with the occurrence of high-temperature extremes and heat wave events over the last few years.

cannot retreat to higher elevations (Bolibar and others, 2022). The lack of topographical feedback from glacier retreat and non-linear response of ice melt and mass balance to increasing air temperatures might be largely relevant on James Ross Archipelago and South Shetland Islands where flat-top glaciers prevail.

Besides the strong vulnerability of ice cap-like glaciers with marine-terminating outlet to rise in ELA, another implication of these glaciers is that mass loss due to frontal ablation is highly variable and sensitive to changes at the ice front (Davies and others, 2012; Dryak and Enderlin, 2020). The rapid retreat of the Davies Dome ice front provides an opportunity to study glacier mass balance during the transition of its calving front to land-terminating terminus. A scarcity of direct observations makes it difficult to predict the timing of this transition. However, persistent retreat of ice front since the 2010s suggests that it could take place within years. Once the terminus recedes out of the sea, a decrease in retreat rate and mass loss can be expected. This change, however, remains poorly known making the future mass balance of ice caps with marine-terminating outlets uncertain. These glaciers prevail in Antarctic periphery and frequently occur in Alaska, Greenland and other Arctic regions.

The observed change in SMB trends in the mid-2010s and subsequent increases in the rate of ice loss confirms that small glaciers are highly sensitive to changes in air temperature. This sensitivity has been demonstrated by recently accelerated retreat of small ice bodies across the glacierized regions including those with similar climate settings (Hugonnet and others, 2021). The accelerated rate of ice loss of these glaciers increases mass deficit exceeding the predicted mass changes and the associated sea-level rise (e.g. Edwards and others, 2021; Rounce and others, 2023). The potential contribution of small glaciers to sea-level rise is limited (Bahr and Radić, 2012; Marzeion and others, 2020), but a further increase in their mass loss would accelerate their dynamic mass loss. Consequently, this would decrease their longevity and result in a higher than expected rate of sea-level rise (Marzeion and others, 2020; Edwards and others, 2021).

check of our manuscript. Finally, we thank Francisco Navarro and an anonymous referee for their thorough reviews and scientific editor Ali Graham for his constructive comments.

References

Abram NJ and 8 others (2013) Acceleration of snow melt in an Antarctic Peninsula ice core during the twentieth century. *Nature Geoscience* **6**(5), 404–411. doi: 10.1038/ngeo1787

Ambrožová K, Láska K, Hrbáček F, Kavan J and Ondruch J (2019) Air temperature and lapse rate variation in the ice-free and glaciated areas of northern JRI, Antarctic Peninsula, during 2013–2016. *International Journal of Climatology* **38**(2), 643–657. doi: 10.1002/joc.5832

Ambrožová K, Láska K and Kavan J (2020) Multi-year assessment of atmospheric circulation and impacts on air temperature variation on James Ross Island, Antarctic Peninsula. *International Journal of Climatology* **40**(3), 1526–1541. doi: 10.1002/joc.6285

Anesio AM and Laybourn-Parry J (2012) Glaciers and ice sheets as a biome. *Trends in Ecology & Evolution* **27**(4), 219–225. doi: 10.1016/j.tree.2011.09.012

Bahr DB and Radić V (2012) Significant contribution to total mass from very small glaciers. *The Cryosphere* **6**, 763–770. doi: 10.5194/tc-6-763-2012

Bolibar J, Rabatel A, Gouttevin I, Zekollari H and Galiez C (2022) Nonlinear sensitivity of glacier mass balance to future climate change unveiled by deep learning. *Nature Communications* **13**, 409. doi: 10.1038/s41467-022-28033-0

Braun M and Hock R (2004) Spatially distributed surface energy balance and ablation modelling on the ice cap of King George Island (Antarctica). *Global and Planetary Change* **42**(1–4), 45–58. doi: 10.1016/j.gloplacha.2003.11.010

Burton-Johnson A, Black M, Fretwell PT and Kaluza-Gilbert J (2016) An automated methodology for differentiating rock from snow, clouds and sea in Antarctica from Landsat 8 imagery: a new rock outcrop map and area estimation for the entire Antarctic continent. *The Cryosphere* **10**, 1665–1677. doi: 10.5194/tc-10-1665-2016

Carrasco JF and Cordero RR (2020) Analyzing precipitation changes in the northern tip of the Antarctic Peninsula during the 1970–2019 period. *Atmosphere* **11**(12), 1270. doi: 10.3390/atmos11121270

Carrasco JF, Bozkurt D and Cordero RR (2021) A review of the observed air temperature in the Antarctic Peninsula. Did the warming trend come back after the early 21st hiatus? *Polar Science* **28**, 100653. doi: 10.1016/j.polar.2021.100653

Carrivick JL, Davies BJ, Glasser NF, Nývlt D and Hambrey MJ (2012) Late-Holocene changes in character and behaviour of land-terminating glaciers on James Ross Island, Antarctica. *Journal of Glaciology* **58**(212), 1176–1190. doi: 10.3189/2012JoG11J148

Cogley JG and 10 others (2011) *Glossary of Glacier Mass Balance and Related Terms*, 1st Edn. Paris: UNESCO-IHP. doi: 10.1657/1938-4246-44.2.256B

Cook AJ, Vaughan DG, Luckman AJ and Murray T (2014) A new Antarctic Peninsula glacier basin inventory and observed area changes since the 1940s. *Antarctic Science* **26**, 614–624. doi: 10.1017/S0954102014000200

Czech Geological Survey (2009) *James Ross Island – Northern Part. Topographic Map 1: 25,000*. Praha: Czech Geological Survey.

Davies BJ, Carrivick JL, Glasser NF, Hambrey MJ and Smellie JL (2012) Variable glacier response to atmospheric warming, northern Antarctic Peninsula, 1988–2009. *The Cryosphere* **6**, 1031–1048. doi: 10.5194/tc-6-1031-2012

Davies BJ and 8 others (2014) Modelled glacier response to centennial temperature and precipitation trends on the Antarctic Peninsula. *Nature Climate Change* **4**, 993–998. doi: 10.1038/nclimate2369

de Smith MJ, Goodchild MF and Longley PA (2015) *Geospatial Analysis. A Comprehensive Guide to Principles, Techniques and Software Tools*, 5th Edn. Winchelsea: Winchelsea Press.

de Woul M and Hock R (2005) Static mass-balance sensitivity of Arctic glaciers and ice caps using a degree-day approach. *Annals of Glaciology* **42**, 217–224. doi: 10.3189/172756405781813096

Dryak MC and Enderlin EM (2020) Analysis of Antarctic Peninsula glacier frontal ablation rates with respect to iceberg melt-inferred variability in ocean conditions. *Journal of Glaciology* **66**(257), 457–470. doi: 10.1017/jog.2020.21

Edwards TL and 83 others (2021) Projected land ice contributions to twenty-first-century sea level rise. *Nature* **593**, 74–82. doi: 10.1038/s41586-021-03302-y

Engel Z, Nývlt D and Láska K (2012) Ice thickness, areal and volumetric changes of Davies Dome and Whisky Glacier, James Ross Island, Antarctic Peninsula in 1979–2006. *Journal of Glaciology* **58**(211), 904–914. doi: 10.3189/2012JoG11J156

Engel Z, Láska K, Nývlt D and Stachoň Z (2018) Surface mass balance of small glaciers on James Ross Island, north-eastern Antarctic Peninsula, during 2009–2015. *Journal of Glaciology* **64**(245), 349–361. doi: 10.1017/jog.2018.17

Engel Z, Kropáček J and Smolíková J (2019) Surface elevation changes on Lachman Crags ice caps (north-eastern Antarctic Peninsula) since 1979 indicated by DEMs and ICESat data. *Journal of Glaciology* **65**(251), 410–421. doi: 10.1017/jog.2019.19

Engel Z, Láska K, Matějka M and Nedělčev O (2022) Effect of geotextile cover on snow & ice ablation on Triangular Glacier, the north-eastern Antarctic Peninsula. *Czech Polar Reports* **12**(2), 256–268. doi: 10.5817/CPR2022-2-19

Engel Z, Láska K, Kavan J and Smolíková J (2023) Persistent mass loss of Triangular Glacier, James Ross Island, north-eastern Antarctic Peninsula. *Journal of Glaciology* **69**(273), 27–39. doi: 10.1017/jog.2022.42

González-Herrero S, Barriopedro D, Trigo RM, López-Bustins JA and Oliva M (2022) Climate warming amplified the 2020 record-breaking heatwave in the Antarctic Peninsula. *Communications Earth & Environment* **3**(1), 122. doi: 10.1038/s43247-022-00450-5

Hawes I and Brazier P (1991) Freshwater stream ecosystems of James Ross Island, Antarctica. *Antarctic Science* **3**(3), 265–271. doi: 10.1017/S0954102091000329

Hock R (2003) Temperature index melt modelling in mountain areas. *Journal of Hydrology* **282**(1–4), 104–115. doi: 10.1016/S0022-1694(03)00257-9

Howat IM, Porter C, Smith BE, Noh MJ and Morin P (2019) The reference elevation model of Antarctica. *The Cryosphere* **13**, 665–674. doi: 10.5194/tc-13-665-2019

Hugonnet R and 10 others (2021) Accelerated global glacier mass loss in the early twenty-first century. *Nature* **592**, 726–731. doi: 10.1038/s41586-021-03436-z

Huss M (2013) Density assumptions for converting geodetic glacier volume change to mass change. *The Cryosphere* **7**, 877–887. doi: 10.5194/tc-7-877-2013

Huss M and Fischer M (2016) Sensitivity of very small glaciers in the Swiss Alps to future climate change. *Frontiers in Earth Science* **4**, 34. doi: 10.3389/feart.2016.00034

Huss M, Bauder A and Funk M (2009) Homogenization of longterm mass-balance time series. *Annals of Glaciology* **50**(50), 198–206. doi: 10.3189/172756409787769627

Jennings SJA and 8 others (2021) Geomorphology of Ulu Peninsula, James Ross Island, Antarctica. *Journal of Maps* **17**(2), 125–139. doi: 10.1080/17445647.2021.1893232

Jones ME and 6 others (2019) Sixty years of widespread warming in the southern mid- and high-latitudes (1957–2016). *Journal of Climate* **32**, 6875–6898. doi: 10.1175/JCLI-D-18-0565.1

Jonsell UY, Navarro FJ, Bañón M, Lapazaran JJ and Otero J (2012) Sensitivity of a distributed temperature-radiation index melt model based on AWS observations and surface energy balance fluxes, Hurd Peninsula glaciers, Livingston Island, Antarctica. *The Cryosphere* **6**(3), 539–552. doi: 10.5194/tc-6-539-2012

Joughin I, Shapero D, Smith B, Dutrieux P and Barham M (2021) Ice-shelf retreat drives recent Pine Island Glacier speedup. *Science Advances* **7**(24), eabg3080. doi: 10.1126/sciadv.abg3080

Jung H, Jeen S-W, Lee H and Lee J (2022) Diel variations in chemical and isotopic compositions of a stream on King George Island, Antarctica: implications for hydrologic pathways of meltwater. *Science of the Total Environment* **825**(15), 153784. doi: 10.1016/j.scitotenv.2022.153784

Kaplan-Pastíriková L, Hrbáček F, Uxa T and Láska K (2023) Permafrost table temperature and active layer thickness variability on James Ross Island, Antarctic Peninsula, in 2004–2021. *Science of the Total Environment* **869**, 161690. doi: 10.1016/j.scitotenv.2023.161690

Kavan J, Nývlt D, Láska K, Engel Z and Kňažková M (2020) High-latitude dust deposition in snow on the glaciers of James Ross Island, Antarctica. *Earth Surface Processes and Landforms* **45**(7), 1569–1578. doi: 10.1002/esp.v45.710.1002/esp.4831

Kavan J, Nedbalová L, Nývlt D, Čejka T and Lirio J (2021) Status and short-term environmental changes of lakes in the area of Devil's Bay, Vega Island, Antarctic Peninsula. *Antarctic Science* **33**(2), 150–164. doi: 10.1017/S0954102020000504

Lapazaran JJ, Otero J, Martín-Español A and Navarro FJ (2016a) On the errors involved in ice-thickness estimates I: ground-penetrating radar measurement errors. *Journal of Glaciology* **62**(236), 1008–1020. doi: 10.1017/jog.2016.93

Lapazaran JJ, Otero J, Martín-Español A and Navarro FJ (2016b) On the errors involved in ice-thickness estimates II: errors in digital elevation models of ice thickness. *Journal of Glaciology* **62**(236), 1021–1029. doi: 10.1017/jog.2016.94

Lippl S and 5 others (2019) Spatial and temporal variability of glacier surface velocities and outlet areas on James Ross Island, Northern Antarctic Peninsula. *Geosciences* **9**, 1–34. doi: 10.3390/geosciences9090374

MALÅ GeoScience (2005) *Ramac GPR. Hardware Manual*. Malå: MALÅ GeoScience.

Marinsek S and Ermolin E (2015) 10 Year mass balance by glaciological and geodetic methods of Glaciar Bahía del Diablo, Vega Island, Antarctic Peninsula. *Annals of Glaciology* **56**(70), 141–145. doi: 10.3189/2015AoG70A958

Marshall GJ and Thompson DWJ (2016) The signatures of large-scale patterns of atmospheric variability in Antarctic surface temperatures. *Journal of Geophysical Research – Atmospheres* **121**, 3276–3289. doi: 10.1002/2015JD024665

Martín-Español A, Lapazaran JJ, Otero J and Navarro FJ (2016) On the errors involved in ice-thickness estimates III: error in volume. *Journal of Glaciology* **62**(236), 1030–1036. doi: 10.1017/jog.2016.95

Marzeion B and 16 others (2020) Partitioning the uncertainty of ensemble projections of global glacier mass change. *Earth's Future* **8**, e2019EF001470. doi: 10.1029/2019EF001470

Matějka M and Láska K (2022) Impact of the selected boundary layer schemes and enhanced horizontal resolution on the Weather Research and Forecasting model performance on James Ross Island, Antarctic Peninsula. *Czech Polar Reports* **12**(1), 15–30. doi: 10.5817/CPR2022-1-2

Mlčoch B, Nývlt D and Mixa P (2019) *Geological Map of James Ross Island – Northern Part 1:25 000*. Praha: Czech Geological Survey.

Narod BB and Clarke GKC (1994) Miniature high-power impulse transmitter for radio-echo sounding. *Journal of Glaciology* **40**(134), 190–194. doi: 10.3189/S002214300000397X

Navarro FJ, Jonsell UY, Corcuera MI and Martín-Español A (2013) Decelerated mass loss of Hurd and Johnsons Glaciers, Livingston Island, Antarctic Peninsula. *Journal of Glaciology* **59**(213), 115–128. doi: 10.3189/2013JoG12J144

Navarro FJ and 8 others (2023). Surface mass balance monitoring of the peripheral glaciers of the Antarctic Peninsula in the context of regional climate change. *Annals of Glaciology* **63**(87–89), 101–106. doi: 10.1017/aog.2023.18

Oliva M and 7 others (2017) Recent regional climate cooling on the Antarctic Peninsula and associated impacts on the cryosphere. *Science of the Total Environment* **580**, 210–223. doi: 10.1016/j.scitotenv.2016.12.030

Osmanoğlu B, Navarro FJ, Hock R, Braun M and Corcuera MI (2014) Surface velocity and mass balance of Livingston Island ice cap, Antarctica. *The Cryosphere* **8**, 1807–1823. doi: 10.5194/tc-8-1807-2014

Palerme C and 5 others (2017) Evaluation of current and projected Antarctic precipitation in CMIP5 models. *Climate Dynamics* **48**(1–2), 225–239. doi: 10.1007/s00382-016-3071-1

Parkinson CL (2019) A 40-y record reveals gradual Antarctic sea ice increases followed by decreases at rates far exceeding the rates seen in the Arctic. *The Proceedings of the National Academy of Sciences* **116**(29), 14414–14423. doi: 10.1073/pnas.1906556116

Pavlis NK, Holmes SA, Kenyon SC and Factor JK (2012) The development and evaluation of the Earth Gravitational Model 2008 (EGM2008). *Journal of Geophysical Research* **117**, B04406. doi: 10.1029/2011JB008916

Rounce DR and 12 others (2023) Global glacier change in the 21st century: every increase in temperature matters. *Science* **379**, 78–83. doi: 10.1126/science.abo1324

Ruiz-Fernández J and 10 others (2019) Patterns of spatio-temporal paraglacial response in the Antarctic Peninsula region and associated ecological implications. *Earth-Science Reviews* **192**, 379–402. doi: 10.1016/j.earscirev.2019.03.014

Silva AB and 5 others (2020) Spatial and temporal analysis of changes in the glaciers of the Antarctic Peninsula. *Global and Planetary Change* **184**, 103079. doi: 10.1016/j.gloplacha.2019.103079

Simões JC, Dani N, Bremer UF, Aquino FE and Arigony-Neto J (2004) Small cirque glaciers retreat on Keller Peninsula, Admiralty Bay, King George Island, Antarctica. *Pesquisa Antártica Brasileira* **4**, 49–56.

Skvarca P, Rott H and Nagler T (1995) Satellite imagery, a baseline for glacier variation study on James Ross Island, Antarctica. *Annals of Glaciology* **21**, 291–296. doi: 10.3189/S0260305500015962

Skvarca P, De Angelis H and Ermolin E (2004) Mass balance of 'Glaciar Bahía del Diablo', Vega Island, Antarctic Peninsula. *Annals of Glaciology* **39**, 209–213. doi: 10.3189/172756404781814672

Surawy-Stepney T, Hogg AE, Cornford SL and Davison BJ (2023) Episodic dynamic change linked to damage on the Thwaites Glacier Ice Tongue. *Nature Geoscience* **16**, 37–43. doi: 10.1038/s41561-022-01097-9

Tuckett PA and 6 others (2019) Rapid accelerations of Antarctic Peninsula outlet glaciers driven by surface melt. *Nature Communications* **10**, 4311. doi: 10.1038/s41467-019-12039-2

Turner J and 8 others (2004) The SCAR READER project: towards a high-quality database of mean Antarctic meteorological observations. *Journal of Climate* **17**(14), 2890–2898. doi: 10.1175/1520-0442(2004)017<2890:TSRPTA>2.0.CO;2

Turner J and 8 others (2005) Antarctic climate change during last 50 years. *International Journal of Climatology* **25**, 279–294. doi: 10.1002/joc.1130

Turner J and 9 others (2016) Absence of 21st century warming on Antarctic Peninsula consistent with natural variability. *Nature* **535**(7612), 411–415. doi: 10.1038/nature18645

Turner J and 5 others (2020) Antarctic temperature variability and change from station data. *International Journal of Climatology* **40**, 2986–3007. doi: 10.1002/joc.6378

van Wessem JM and 10 others (2016) The modelled surface mass balance of the Antarctic Peninsula at 5.5 km horizontal resolution. *The Cryosphere* **10**, 271–285. doi: 10.5194/tc-10-271-2016

Vaughan DG and 8 others (2003) Recent rapid regional climate warming on the Antarctic Peninsula. *Climate Change* **60**, 243–274. doi: 10.1023/A:1026021217991

Wallis BJ, Hogg AE, van Wessem JM, Davison BJ and van den Broeke MR (2023) Widespread seasonal speed-up of west Antarctic Peninsula glaciers from 2014 to 2021. *Nature Geoscience* **16**, 231–237. doi: 10.1038/10.1038/s41561-023-01131-4

WGMS (2021) *Fluctuations of Glaciers Database*. Zurich: World Glacier Monitoring Service. Online access: doi: 10.5904/wgms-fog-2021-05

WGMS (2023) Global Glacier Change Bulletin No. 5 (2020-2021). Zemp M, Gärtner-Roer I, Nussbaumer SU, Welty EZ, Dussaillant I and Bannwart J (eds.), ISC (WDS)/IUGG (IACS)/UNEP/UNESCO/WMO, Zurich, Switzerland: World Glacier Monitoring Service, 134 pp., publication based on database version doi: 10.5904/wgms-fog-2023-09.

Zheng L, Zhou C and Liang Q (2019) Variations in Antarctic Peninsula snow liquid water during 1999–2017 revealed by merging radiometer, scatterometer and model estimations. *Remote Sensing of Environment* **232**, 111219. doi: 10.1016/j.rse.2019.111219

Zhou C, Liu Y and Zheng L (2021) Satellite-derived dry-snow line as an indicator of the local climate on the Antarctic Peninsula. *Journal of Glaciology* **68**, 54–64. doi: 10.1017/jog.2021.72